Monitoring urban land cover change: An expert system approach to land cover classification of semiarid to arid urban centers

William L. Stefanov[a,b,*], Michael S. Ramsey[c,1], Philip R. Christensen[a,2]

[a]*Department of Geological Sciences, Arizona State University, Tempe, AZ 85287, USA*
[b]*Center for Environmental Studies, Arizona State University, Tempe, AZ 85287, USA*
[c]*Department of Geology and Planetary Science, University of Pittsburgh, Pittsburgh, PA, USA*

Abstract

The spatial and temporal distribution of land cover is a fundamental dataset for urban ecological research. An expert (or hypothesis testing) system has been used with Landsat Thematic Mapper (TM) data to derive a land cover classification for the semiarid Phoenix metropolitan portion of the Central Arizona-Phoenix Long Term Ecological Research (CAP LTER) site. Expert systems allow for the integration of remotely sensed data with other sources of georeferenced information such as land use data, spatial texture, and digital elevation models (DEMs) to obtain greater classification accuracy. Logical decision rules are used with the various datasets to assign class values to each pixel. TM reflectance data acquired in 1998 [visible to shortwave infrared (VSWIR) bands plus a vegetation index] were initially classified for land cover using a maximum likelihood decision rule. In addition, spatial texture of the TM data was calculated. An expert system was constructed to perform postclassification sorting of the initial land cover classification using additional spatial datasets such as texture, land use, water rights, city boundaries, and Native American reservation boundaries. Pixels were reclassified using logical decision rules into 12 classes. The overall accuracy of this technique was 85%. Individual class user's accuracy ranged from 73% to 99%, with the exception of the commercial/industrial materials class. This class performed poorly (user's accuracy of 49%) due to the similarity of subpixel components with other classes. The results presented here indicate that the expert system approach will be useful both for ongoing CAP LTER research, as well as the planned global Urban Environmental Monitoring (UEM) program of the Advanced Spaceborne Thermal Emission and Reflection Radiometer (ASTER) instrument. © 2001 Elsevier Science Inc. All rights reserved.

Keywords: Arid environment; Knowledge-based systems; Surface properties; Thematic mapper; Urban environment

1. Introduction

Urban land cover types and their areal distributions are fundamental data required for a wide range of studies in the physical and social sciences, as well as by municipalities for land planning purposes. The visible to shortwave infrared (VSWIR) bands of Landsat Multispectral Scanner (MSS) and Thematic Mapper (TM) data have been extensively used for forestry and agricultural land cover analysis since the Landsat program began in 1972 (an extensive literature exists; some examples are Anderson, Hardy, Roach, & Witmer, 1976; Botkin, Estes, & MacDonald, 1984; Lorenzo-Garcia & Hoffer, 1993; Pax-Lenney & Woodcock, 1997; Wilkie & Finn, 1996). Urban land cover analysis has also made extensive use of the MSS and TM scanners (Haack, 1983; Haack, Bryant, & Adams, 1987; Lindgren, 1985; Ridd, 1995; Ridd & Liu, 1998). However, the relatively low resolution of the MSS (79 m/pixel) and TM (28.5 m/pixel) data only allows classification of land cover to Level 1–2 of the Anderson system (Anderson et al., 1976; Ridd, 1995). New sensors with higher spatial resolutions are also being used for urban studies and allow a land cover classification to Level 2–3 of Anderson et al. (1976). These instruments include the 10–20 m/pixel SPOT

* Corresponding author. Department of Geological Sciences, Arizona State University, Tempe, AZ 85287, USA. Fax: +1-480-965-1787.

E-mail address: will.stefanov@asu.edu (W.L. Stefanov).
[1] Fax: +1-412-624-3914.
E-mail address: mramsey+@pitt.edu (M.S. Ramsey)
[2] Fax: +1-480-965-1787.
E-mail address: phil.christensen@asu.edu (P.R. Christensen).

(Gong & Howarth, 1990; Martin, Howarth, & Holder, 1988; Ridd, 1995; Treitz, 1992), as well as airborne scanners with 3–15 m/pixel resolution such as the Thermal Infrared Multispectral Scanner (TIMS) and the TM simulator (NS001) (Quattrochi & Ridd, 1998; Ramsey, Stefanov, & Christensen, 1999). Newer sensors with either greater spectral/temporal resolution such as the Advanced Spaceborne Thermal Emission and Reflection Radiometer (ASTER), the Enhanced TM Plus (ETM+), the airborne MODIS/ASTER simulator (MASTER), or increased (1 m/pixel or less) spatial resolution (Ikonos) will allow even more precise land cover classification. Data collected by the MSS and TM will continue to be used as a historical global database. The work presented here uses TM data. However, the basic technique is applicable to any remotely sensed data, and should improve in accuracy with increased spectral and/or spatial resolution of those data.

The majority of studies relying on remotely sensed information to classify land cover types either use raw data number (DN) values or calibrated reflectance (R_o), if a more precise material identification is needed. Geological and biological applications of TM data have also used simple band ratio techniques and spectroscopy to accentuate spectral features indicative of specific surficial materials, biomass, and vegetation health (Huete, 1988; Lyon, Yuan, Lunetta, & Elvidge, 1998; Mattikalli, 1997; Sultan, Arvidson, Sturchio, & Guinness, 1987). Land cover classification of urban areas has been problematic due to the heterogeneity and small spatial size of the surficial materials, which leads to significant subpixel mixing (Foody, 2000; Ridd, 1995). This problem becomes exacerbated when discrimination of multiple classes is necessary. Significant improvements in the accuracy of land cover classification in urban areas have been achieved using a variety of sophisticated approaches including: (1) the use of neural networks (Berberoglu, Lloyd, Atkinson, & Curran, 2000; Kumar, Basu, & Majumdar, 1997; Paola & Schowengerdt, 1995); (2) fuzzy classification (Bastin, 1997; Fisher & Pathirana, 1990; Foody, 2000); and (3) image texture analysis (Berberoglu et al., 2000; Gong & Howarth, 1990; Iron & Petersen, 1981; Stuckens, Coppin, & Bauer, 2000).

Yet another successful technique for improving classification accuracy has been the incorporation of other data sources in a classification or postclassification sorting mode, referred to hereafter as an expert system (Cibula & Nyquist, 1987; Franklin, 1994; Greenberg & Bradley, 1997; Harris & Ventura, 1995; Loveland, Merchant, Ohlen, & Brown, 1991; Stuckens et al., 2000; Treitz, 1992; Vogelmann, Sohl, & Howard, 1998). Harris & Ventura (1995) used zoning and housing density information to perform postclassification sorting of an initial maximum likelihood classification of TM data for the Beaver Dam, Wisconsin area. Vogelmann et al. (1998) incorporated vegetation indices derived from their base TM data, together with several ancillary datasets, to produce a final land cover classification of a 30 million ha region in the eastern United States. Greenberg and Bradley (1997) used population and road density information with TM data to classify land cover in the Seattle, WA area. Stuckens et al. (2000) produced a land cover classification of the Minneapolis-St. Paul, MN urban area using TM data with ancillary land use and wetland inventory information.

The present work applies an expert system approach to the semiarid urban land cover of Maricopa County, AZ. The study area occupies approximately 7900 km^2 centered on the Phoenix, AZ metropolitan region (Fig. 1). Urban and suburban development of the study region has proceeded at a high rate with widespread conversion of adjacent, undeveloped desert regions and agricultural lands to residential and commercial uses. The county has been ranked as the first or second fastest growing region in the United States since 1990. Data collected in 1995 (Maricopa Association of Governments, 1995) indicated that the Phoenix metropolitan area included 1168 km^2 in residential use, 378 km^2 in urban (commercial, industrial, and public facilities) use, 2424 km^2 in agricultural (and vacant) use, and 448 km^2 of open space. The primary motivation for this work is historical land cover classification and future monitoring of land cover change as part of the Central Arizona-Phoenix Long Term Eco-
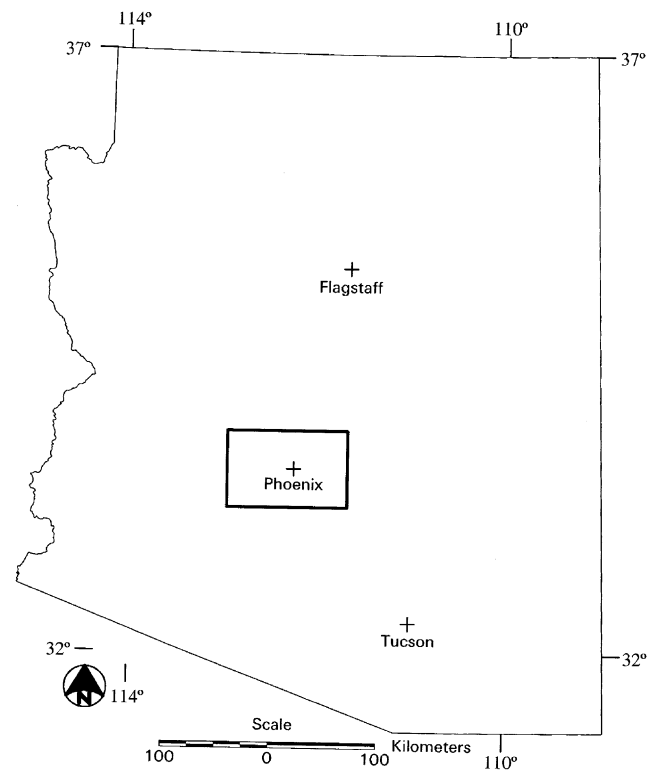

Fig. 1. Location map for the metropolitan Phoenix, AZ study region (black rectangle). The locations of major urban centers in Arizona are provided for geographic reference.

logical Research (CAP LTER) Project. In addition, techniques such as those presented here will be applied to data collected by the ASTER instrument over 100 of the world's largest and most at-risk urban centers to map land cover and assess its temporal variability over 6 years.

2. Methodology

2.1. Data processing and atmospheric correction

Two adjacent scenes of TM data were required to completely cover the Phoenix metropolitan region (acquired May 24, 1998 and June 18, 1998). Each TM scene was georeferenced to the NAD27 datum and Universal Transverse Mercator Zone 12 North coordinate system with an estimated positional error of 0.3–0.5 pixel, or 9–15 m. The NAD27 datum was selected to match the geographic projections of the ancillary datasets. The two scene histograms were compared to assess the similarity of

pixel DN distributions. As the histograms were similar, histogram matching was performed prior to any additional processing to minimize interscene variability. A single mosaic image was then constructed from the two histogram-matched scenes. The study area was subset out of the scene mosaic, corrected for the effects of atmosphere, and converted to calibrated reflectance using commercially available software that incorporates the MODTRAN3 radiative transfer code (ATCOR2 for the ERDAS Imagine software; GEOSYSTEMS GmbH, 1997). As the two scenes were collected within 1 month of each other, significant changes in the atmospheric components of scene radiance were not expected. A midlatitude summer, urban aerosol concentration model with 25 km estimated visibility therefore was used as input to the radiative transfer code.

TM VSWIR Bands 1–5 and 7 were combined with a soil-adjusted vegetation index (SAVI) layer calculated from the scene mosaic to minimize shadow effects on subsequent classification. The SAVI is similar to the frequently used
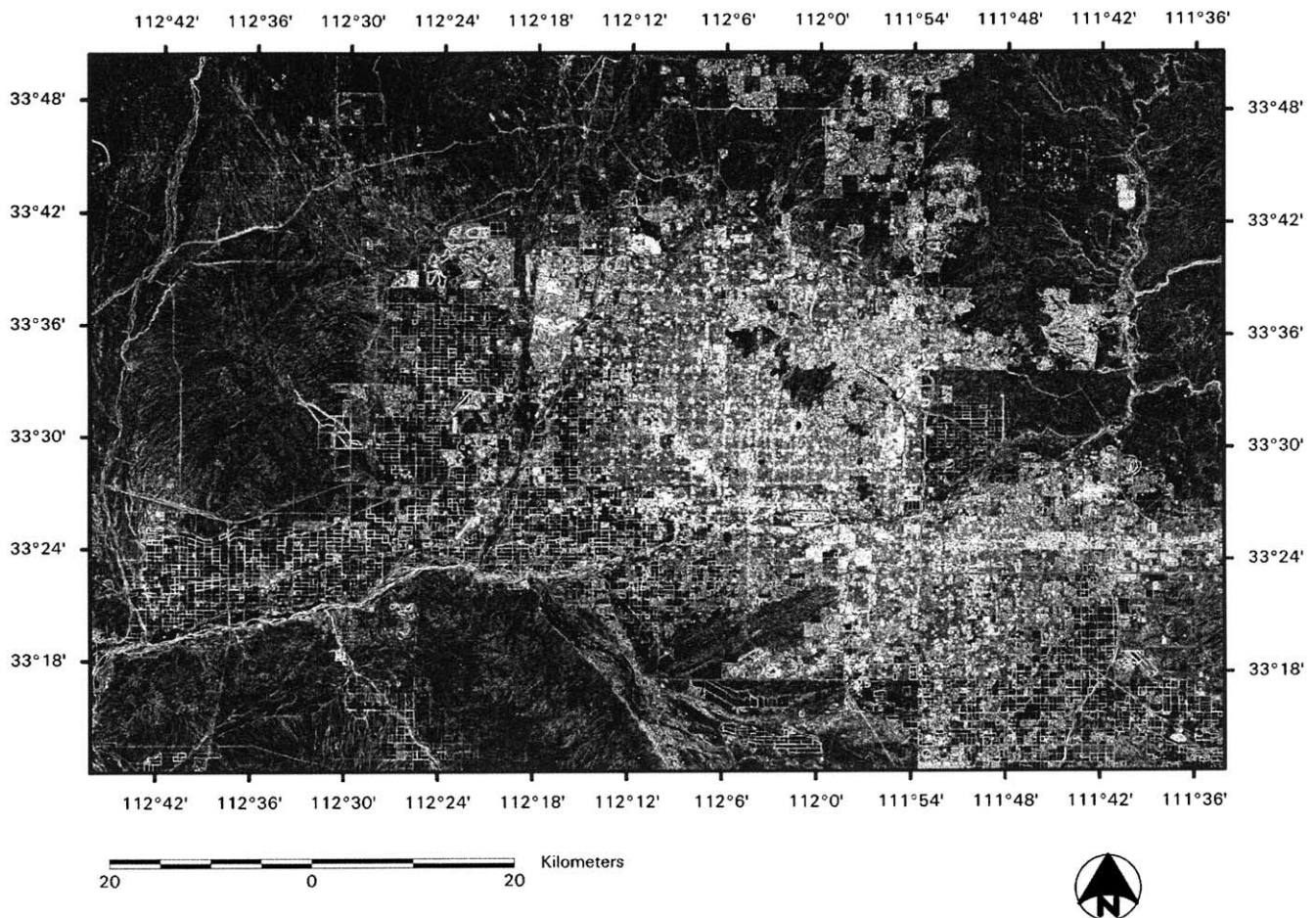

Fig. 2. Texture image of the study region derived from calculating pixel variance using a 3 × 3 moving window [Eqs. (2) and (3) in text]. Regions of high edge density (urbanized areas) appear bright, whereas regions of low edge density (agricultural fields, undeveloped areas) appear dark. Note that natural linear features such as river channels and large rock outcrops are accentuated by the variance texture calculation, but the values of these features are generally intermediate between urban and homogeneous regions.

Normalized Difference Vegetation Index (NDVI) but includes an additional factor to account for soil reflectance such that one obtains [Eq. (1)]:

$$\text{SAVI} = \left[\frac{(\text{NIR} - \text{VISred})}{(\text{NIR} + \text{VISred} + L)}\right](1 + L), \tag{1}$$

where NIR (near infrared) = Band 4; VISred (visible red) = Band 3; and *L*, designed to correct for the soil reflectance component of energy detected by the sensor, is equal to 0.5 (Huete, 1988). As the SAVI is a band ratio, shadow effects are removed in the resulting grayscale image. The resulting seven-band image (VSWIR Bands 1–5 and 7 plus the SAVI for shadow correction) was used as the baseline dataset for generation of an initial land cover classification. Additional datasets used as input into the expert system were a texture image derived from the TM mosaic and several vector coverages for the study region (land use, water rights data, city boundaries, and

reservation boundaries). All coverages were georeferenced to the NAD27, UTM Zone 12 coordinate system and converted to raster images (resampled to the 28.5-m/pixel TM spatial resolution). As it is necessary to understand the nature and potential errors associated with each of these data sources, a brief description of each is presented as follows.

2.2. Texture analysis

The study area is comprised of urbanized, undisturbed, and agricultural regions. These different types of land uses have distinct spatial edge frequencies or texture that can be used as input into classification algorithms (Berberoglu et al., 2000; Gong & Howarth, 1990; Iron & Petersen, 1981; Stuckens et al., 2000). Urban areas typically have significant texture resulting from buildings and street grids, whereas homogeneous areas such as agricultural fields have little to no texture (Fig. 2). Texture values were calculated from the
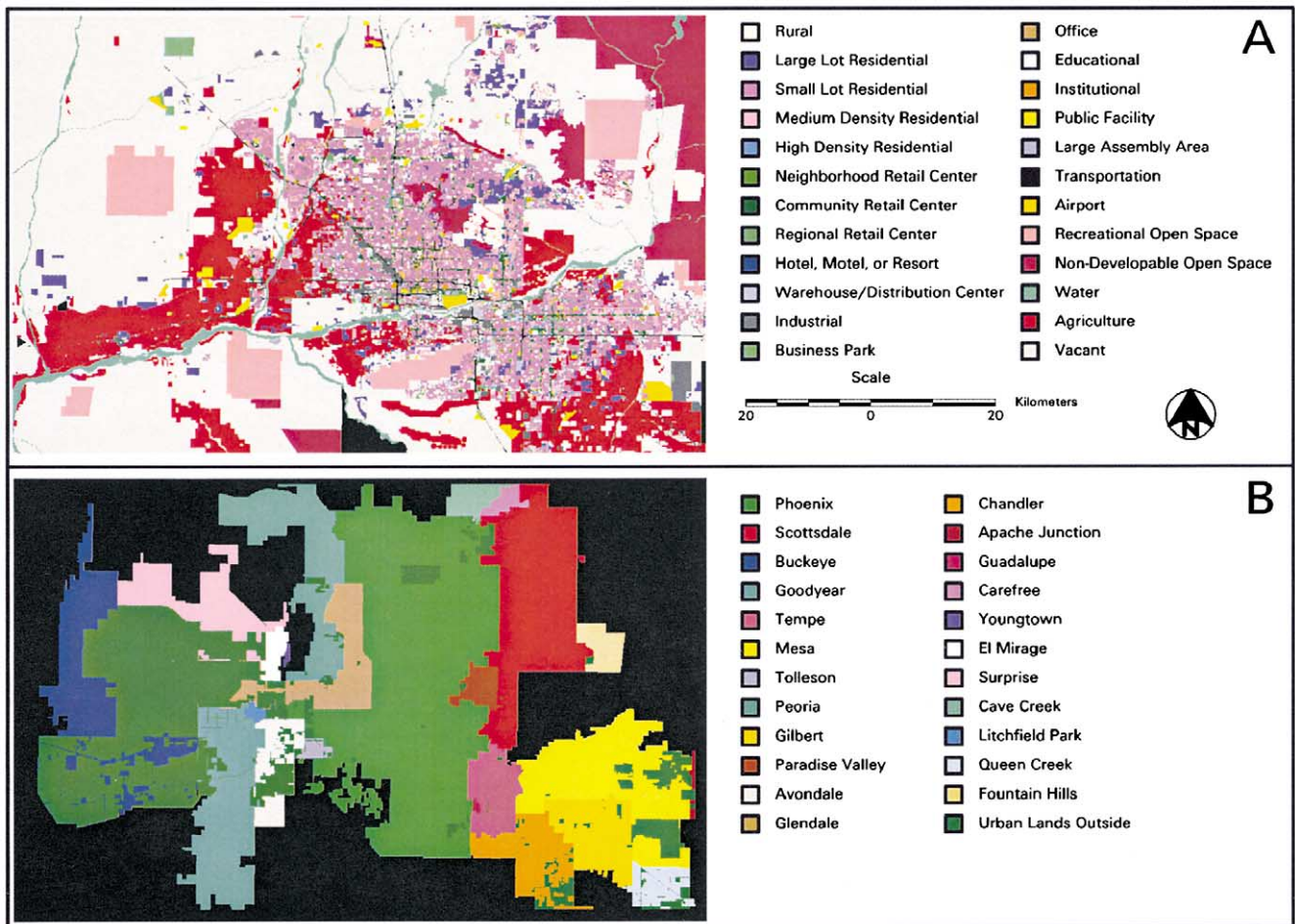

Fig. 3. Several ancillary datasets were used as inputs into the expert system classification. These datasets include land use (A), city boundaries (B), water rights (C), and reservation boundaries (D). Land use data were obtained from the Maricopa Association of Governments, city and reservation boundary data were obtained from the Arizona Land Resource Information System, and water rights data were obtained from the Arizona Department of Water Resources. All datasets were georeferenced to the NAD27, UTM Zone 12 coordinate system. Area of coverage is the same as Fig. 2.
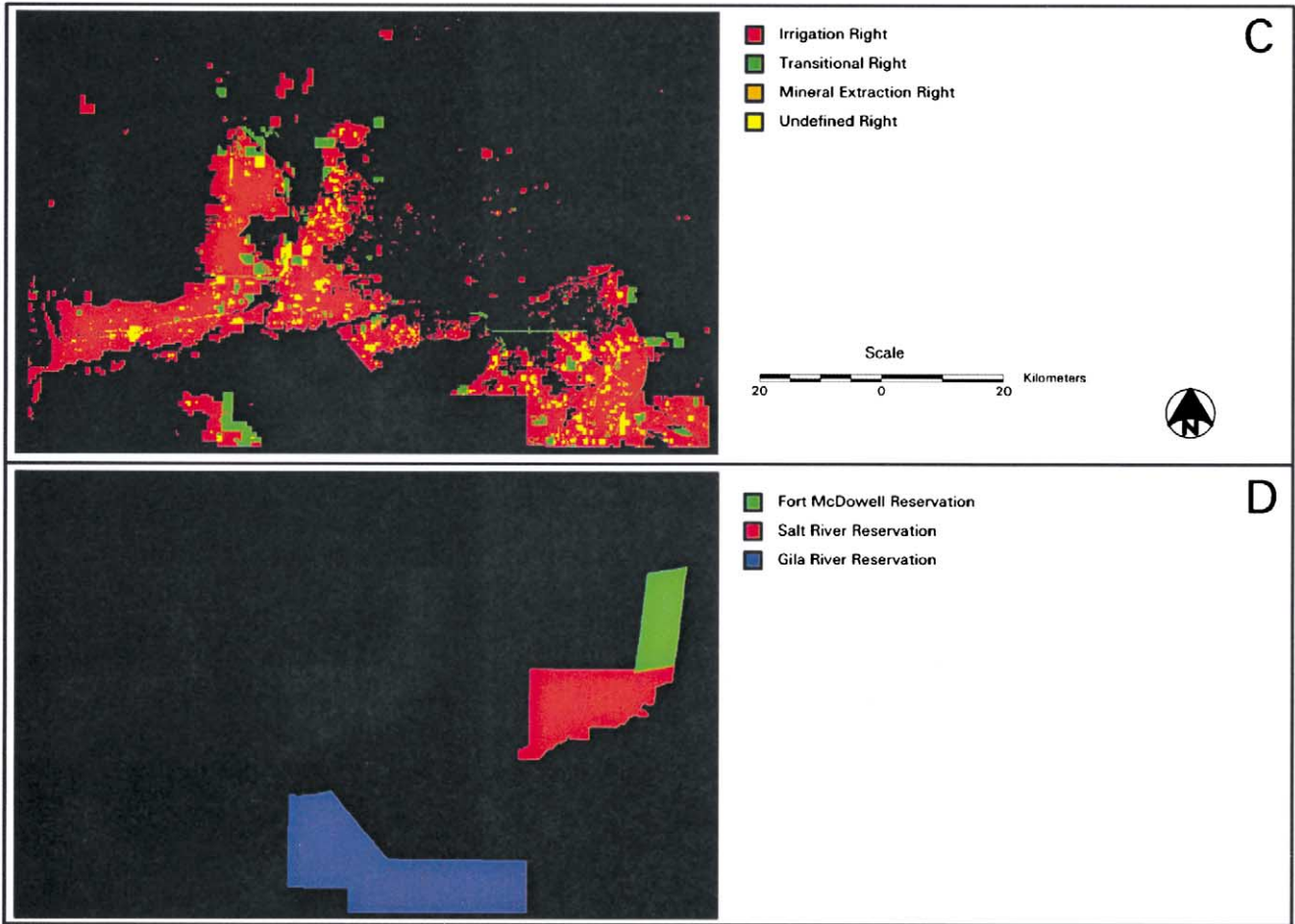
Fig. 3 (*continued*).

TM base data using a 3×3 moving window and the variance [V; Eq. (2)]:

$$V = \sum \frac{(x_{ij} - M)^2}{n - 1} \qquad (2)$$

where x_{ij} = DN value of pixel (i,j); n = number of pixels in moving window; and M is the mean value of the moving window (ERDAS, 1999) and defined as [Eq. (3)]:

$$M = \frac{\sum x_{ij}}{n} \qquad (3)$$

2.3. Land use

Land use information for the study site was obtained as a vector polygon coverage from the Maricopa Association of Governments (1995). Twenty-four classes are defined in this coverage and include residential, industrial, commercial, agricultural, and natural (undisturbed) land uses. The land use data were collected during 1995 and were compiled using site visits, aerial photography, and survey questionnaires sent to commercial and industrial properties. Reported spatial accuracy of the dataset is $\pm \sim 6$ m in developed areas and $\pm \sim 61$ m in rural and undeveloped areas (J. Fry, personal communication).

Land cover types, present in several different land use categories, can cause interpretive difficulties for users of classified data. For example, a vegetation land cover class based on surficial reflectance properties may correspond to residential, vacant, recreational open space, or agricultural land use types. Land use data can also be useful in reclassifying pixels misclassified due to subpixel mixing and edge effects. For example, pixels with a vegetation classification can be reclassified as agricultural vegetation using land use data.

2.4. Water rights

Vegetation abundance (derived from TM data) combined with surficial water rights data can provide accurate classification of active and fallow agricultural regions. The Arizona Department of Water Resources (ADWR) maintains a

database of surface water rights in the study area. This database was first constructed in 1980 using deeds, aerial photography, county assessor data, and field sketches that were subsequently digitized using a GIS. The State of Arizona Groundwater Management Act of 1980 enacted a moratorium on the issuance of new water rights. This limits changes in the database to transferal or abandonment of water rights (usually agricultural) to other land uses such as residential development. The unidirectional change from agricultural to nonagricultural water rights insures that the expert system model is applicable to additional TM data for the study area collected subsequent to 1980.

2.5. City and reservation boundaries

Information on incorporated city boundaries and the locations of Native American reservations were necessary due to spatial gaps in some of the other ancillary datasets. For example, the water use database does not include Native American reservation lands. This led to significant misclassification of cultivated vegetation and compacted soil areas (that were prior agricultural fields) in these regions. Vector data for the city and reservation boundaries [derived from Topographically Integrated Geographic Encoding Reference (TIGER) information] were obtained from the Arizona Land Resource Information System (ALRIS, 1999). Examples of the vector coverages used in the expert system classification are illustrated in Fig. 3.

2.6. Initial image classification

The present work is an expansion of a pilot study for the east-central Phoenix and Tempe, AZ urban area performed for the CAP LTER project (Ramsey et al.,

Table 1
Maximum likelihood rule initial land cover classes

Class	Bayesian coefficient
Vegetation	1.0
Undisturbed	1.0
Water	1.0
Disturbed (mesic residential materials)	1.0
Disturbed (xeric residential materials)	1.0
Disturbed (commercial/industrial materials)	0.25
Disturbed (asphalt + concrete)	0.25
Disturbed (compacted soil)	0.50

1999). The results of this pilot study indicated that several key land cover classes (such as river gravels and asphalt) were confused due to the spectral similarity of these classes (Fig. 4). The number of land cover classes used in the initial pilot study (27) was reduced to eight major classes to reduce misclassification (Table 1). A hard classification of the TM data was then performed using a maximum likelihood decision rule (Jensen, 1996). Bayesian coefficients (weighting factors that reflect the probability of occurrence for a given class in the scene) used in the maximum likelihood classification are presented in Table 1. Lower probabilities were assigned to classes that demonstrated higher degrees of confusion with other, more spatially extensive classes within the scene. These values were somewhat arbitrarily determined based on qualitative estimation of the area each class occupied within the study region.

The initial land cover classes were selected on the basis of spectral separability in TM data and usefulness to the CAP LTER research objectives. Training regions for the land cover classes were determined using ancillary geological, land use, and field data. Each training region consisted of at least 70 image pixels to satisfy the 10 n
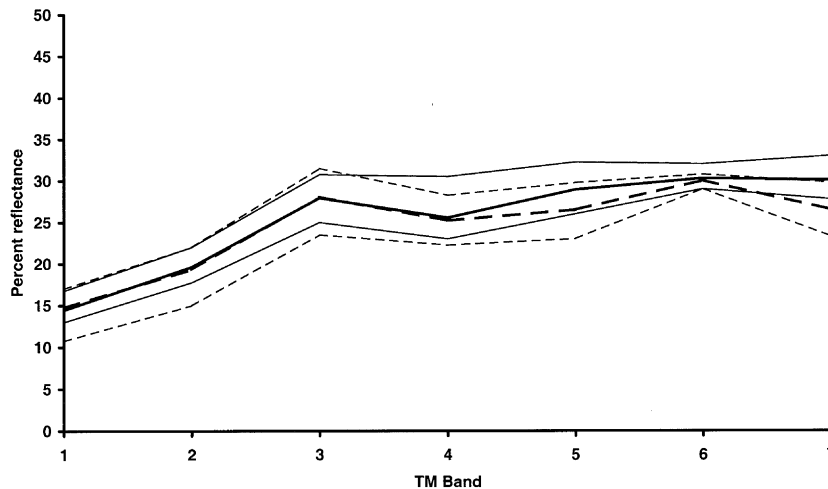

Fig. 4. Land cover classes with significant spectral overlap can be difficult to classify accurately using traditional hard decision rules such as minimum distance or maximum likelihood. For example, asphalt and river gravels within the study region exhibit similar spectral reflectance. The heavy solid line represents the mean reflectance spectrum of 10 randomly selected asphalt-dominated pixels, with the minimum and maximum reflectance envelope represented by thin solid lines. The heavy dashed line represents the mean reflectance spectrum of 10 randomly selected river gravel-dominated pixels, with the minimum and maximum reflectance envelope represented by thin dashed lines. TM Band 6 is comprised of SAVI values.

Table 2
Training region statistics for maximum likelihood classification

| | Water | Undisturbed | Vegetated | Disturbed | | | | |
				Mesic residential	Xeric residential	Commercial/Industrial	Asphalt	Vacant
Pixels	23288	12782945	14402	1656	1215	10024	1302	4118
Reflectance[a]								
Band 1	1.84 ± 0.30	11.88 ± 2.58	5.38 ± 1.93	10.21 ± 2.45	13.34 ± 2.74	14.98 ± 5.86	12.35 ± 3.34	11.37 ± 3.94
Band 2	3.26 ± 0.29	17.92 ± 3.66	8.78 ± 2.71	14.28 ± 2.99	17.82 ± 3.31	63.75 ± 19.84	16.29 ± 4.34	18.78 ± 5.87
Band 3	3.88 ± 0.43	28.86 ± 5.81	12.16 ± 5.02	18.97 ± 4.28	24.83 ± 4.56	28.18 ± 9.02	23.49 ± 5.59	32.82 ± 9.02
Band 4	2.23 ± 0.70	33.97 ± 4.91	34.94 ± 10.81	34.91 ± 3.78	31.30 ± 4.21	28.98 ± 8.10	21.76 ± 4.80	36.41 ± 9.15
Band 5	1.84 ± 0.84	43.87 ± 7.47	23.66 ± 5.20	27.29 ± 3.58	28.67 ± 4.24	30.77 ± 8.04	26.13 ± 4.73	43.71 ± 8.35
Band 6	23.48 ± 2.30	34.46 ± 1.50	46.87 ± 5.45	41.34 ± 2.99	35.46 ± 2.20	32.25 ± 3.10	30.52 ± 1.03	33.44 ± 0.78
Band 7	1.29 ± 1.00	38.39 ± 8.26	14.67 ± 4.44	20.52 ± 3.62	24.56 ± 4.54	29.67 ± 8.51	27.38 ± 5.39	40.45 ± 6.20

[a] Values are Mean Percent Reflectance $\pm 1\sigma$ for TM Bands 1–5 and 7. Band 6 is SAVI calculated from TM reflectance values.

criterion, where $n =$ number of bands used for the classification (Congalton & Green, 1999). Multiple training regions were selected for each class and then merged to ensure a Gaussian distribution of pixel values necessary for application of the maximum likelihood decision rule. Training region statistics were calculated for each class and are presented in Table 2.

2.7. Expert system classification

An expert system classification model was constructed using the ERDAS Imagine image-processing software. The primary motivation behind using the expert system was to reclassify the initial maximum likelihood classification and reduce errors of omission and commission. Use of the expert system also allowed for the assignment of four additional land cover classes [cultivated vegetation, cultivated grass, fluvial and lacustrine sediments (canals), and compacted soil (prior agricultural use)] to the eight classes used in the initial land cover classification. Definitions of the expert system classes are provided in Table 3.

Pixel classifications were determined using a hypothesis-testing framework (Fig. 5). A typical hypothesis would be that a given pixel is comprised of xeric residential materials. For this hypothesis to be true (and for the pixel to receive this classification), a number of conditional statements must be true. For example, if the pixel was initially classified as

xeric residential material, and the pixel is not located within an agricultural water right area, and it is not located within a dedicated/nondevelopable area, and the pixel has a texture value ≥ 10, then the pixel is classified as xeric residential material. The same approach can be used to reclassify pixels that were initially misclassified. This would be the case if a pixel was initially classified as mesic residential material, however, it is located within a dedicated/nondevelopable area and has a texture value < 10. Because of the latter two criteria, the pixel is recoded to the undisturbed class.

3. Results

Initial classification efforts for the Phoenix metropolitan area included a number of trials that varied base image type, classification algorithm, and number of classes. Table 4 ranks these various trials on the basis of their overall accuracy. Inspection of Table 4 indicates that the highest overall classification accuracy (72%) is obtained using a calibrated reflectance (with SAVI in place of the thermal TM band) base image, fuzzy classification rule, and four general classes (water, vegetation, impervious, and soil). It is clear from the classification accuracy results presented in Table 4 that the best performance is obtained using fewer classes and reflectance base data, while the worst performance is obtained using multiple classes and band ratio data alone.

Table 3
Expert system class definitions

| Class	Properties
Cultivated vegetation	Actively photosynthesizing vegetation, with agricultural water rights
Cultivated grass	Actively photosynthesizing vegetation, in urban park areas
Vegetation	Actively photosynthesizing vegetation
Fluvial and lacustrine sediments (canals)	Mixed lithology gravels and soil associated with water transport features
Water	Standing or flowing water
Undisturbed	Undisturbed soil and native vegetation, bedrock outcrops
Compacted soil (prior agricultural use)	Disturbed soil with agricultural water rights
Compacted soil	Disturbed or bladed soil
Disturbed (commercial/industrial)	Mixed asphalt, concrete, soil, vegetation, and building materials, dense spatial texture
Disturbed (asphalt and concrete)	Mixed asphalt and concrete
Disturbed (mesic residential)	Built materials, vegetation cover greater than bare soil; dense spatial texture
Disturbed (xeric residential)	Built materials; vegetation cover less than bare soil; dense spatial texture
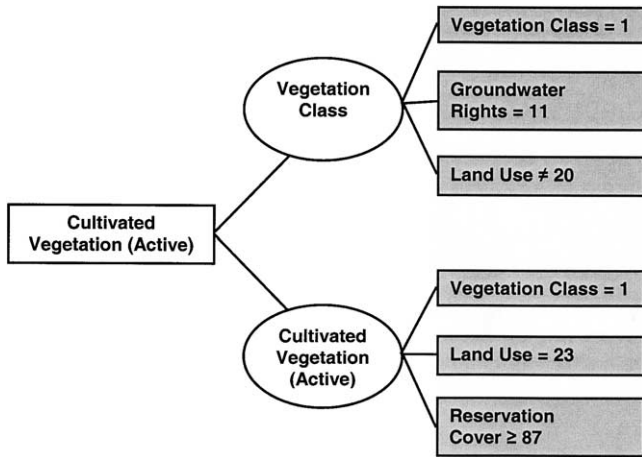
Fig. 5. An expert system was constructed to recode the initial maximum likelihood classification using the additional information provided by the vector coverages. In this example, schematic diagram white boxes represent the hypothesis being tested, white ellipses represent the conjunctive decision rules, and gray boxes represent the variables used (defined as pixel values for the specific data layer) to test the hypothesis. Multiple branches connected to hypotheses indicate exclusive conditional statements.

The four highly generalized classes used in the most accurate classifications (ranked 1–3 in Table 4) are too broad to be useful for the majority of research objectives associated with the CAP LTER or ASTER programs; therefore the expert system technique was developed to increase the number of land cover classes while retaining high classification accuracy.

Fig. 6 presents the land cover classification of the study area produced using the expert system. Classification accuracy was assessed using a reference dataset of 981 randomly selected points for which land cover was determined using a 1999 orthophoto mosaic georeferenced to the TM data. The original TM data were also used in accuracy assessment to avoid introducing errors into the reference dataset for temporally sensitive classes (such as cultivated vegetation). The expert system land cover classification was used to generate 100 random validation points for each output class. A 3×3 moving window with a class majority rule was passed over the output classification to determine validation points. Validation pixels that fell within their own class training regions were removed from the reference dataset.

Likewise, validation points that did not have pixel values equal to the class under inspection (an artifact of the pixel selection method) were discarded. This resulted in a range of 70–100 validation points for each output class. Additional land cover data for the reference dataset were collected by field verification of the classified image.

Both producer's accuracy (the percentage of pixels classified as a particular land cover that actually are that land cover) and user's accuracy (the percentage of reference pixels for a given land cover that are correctly classified) are generally reported. User's accuracy is the more relevant measure of the classification's actual utility in the field. Additional information regarding the error matrix can be obtained using a k analysis that incorporates measures of the omission and commission errors to obtain accuracy values (Jensen, 1996). Producer's, user's, and overall accuracy (and corresponding k analysis values) of the classification were calculated using an error matrix (Congalton & Green, 1999). The results of the accuracy assessment are presented in Table 5.

4. Discussion

4.1. Classification of urban materials

The primary motivation for the construction and implementation of the expert system classification presented here was to improve upon the performance of hard classifiers for the study area. Application of commonly used algorithms such as maximum likelihood and minimum distance did not have encouraging results, with the best performance obtained from classifications with a relatively small number of general classes (59–72% overall accuracy; Table 4). Whereas the use of a simple scheme incorporating generalized classes (water, vegetation, soil, and impervious materials) is useful for first-order comparisons between urban regions (Ridd, 1995), a greater level of land cover discrimination is required for detailed analyses of urban ecosystem processes.

One of the major confounding factors contributing to poor classification accuracy in urban regions is the high degree of heterogeneity and subpixel mixing of surficial

Table 4
Initial classification trial results

Classification rule	Base data[a]	No. of classes	Overall accuracy (%)	Overall k (%)	Rank[b]
Fuzzy classification	VSWIR	4	71.56	53	1
Maximum likelihood	VSWIR	4	69.97	50	2
Minimum distance	Ratio	4	58.82	34	3
Maximum likelihood	VSWIR	8	57.89	43	4
Fuzzy classification	VSWIR	8	56.97	43	5
Maximum likelihood	Ratio	27	23.53	17	6

  [a] Ratio base data are a three-band image derived from TM reflectance: R-(5/7), G-(5/1), B-[(5/4)(3/4)]. VSWIR base data are TM Bands 1–5 and 7 with SAVI index in place of the thermal band (Band 6).
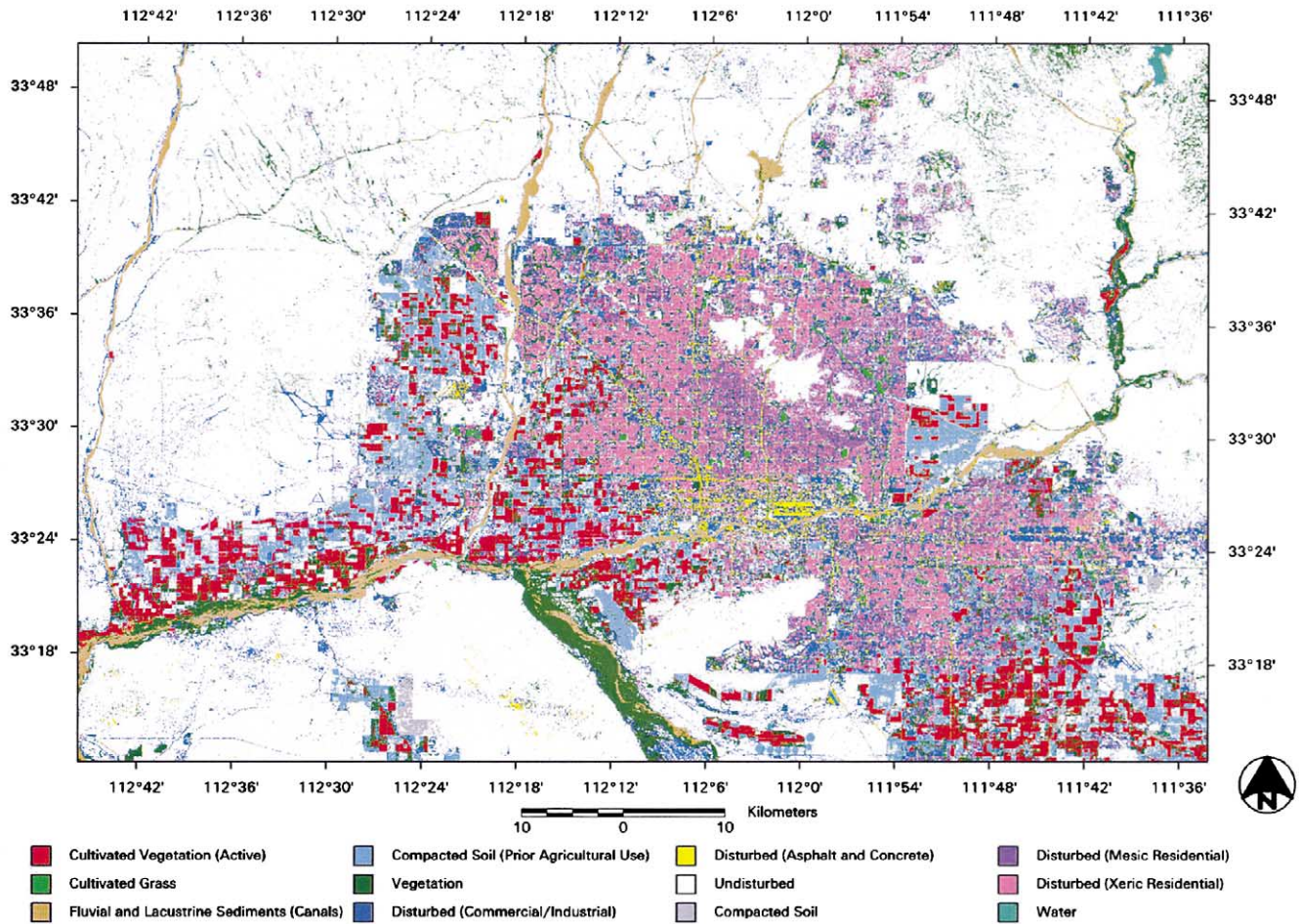 [b] Rank is based on overall accuracy and ranges from one (highest) to six (lowest).

Fig. 6. Recoding the initial maximum likelihood classification using the expert decision rules and ancillary datasets produced the final land cover classification. Use of the expert system also enabled the addition of four new land cover classes to the initial classification [cultivated vegetation, cultivated grass, compacted soil (prior agricultural use) and fluvial and lacustrine sediments (canals)]. Producer's, user's, and overall accuracies (and k coefficients) for the expert system classification are presented in Table 5.

materials at the scale of a Landsat image pixel (Foody, 2000). For example, it is not uncommon for xeric and mesic residential properties to be directly adjacent to each other within the same subdivision in the Phoenix metropolitan area. These residences may also be bordered by a commercial strip center that utilizes similar building and landscap-

Table 5
Accuracy assessment for expert system classification

Class	Reference totals	Classified totals	No. correct	Producer's accuracy (%)	User's accuracy (%)	k (%)
Cultivated vegetation	99	99	93	93.94	93.94	93.26
Cultivated grass	77	78	76	98.70	97.44	97.22
Fluvial and lacustrine sediments (canals)	77	88	72	93.51	81.82	80.27
Compacted soil (prior agricultural use)	81	84	71	87.65	84.52	83.13
Vegetation	80	84	61	76.25	72.62	70.19
Disturbed (commercial/industrial)	54	71	35	64.81	49.30	46.34
Disturbed (asphalt and concrete)	67	71	61	91.04	85.92	84.88
Undisturbed	101	95	86	85.15	90.53	89.44
Compacted soil	110	87	83	75.45	95.40	94.82
Disturbed (mesic residential)	70	72	59	84.29	81.94	80.56
Disturbed (xeric residential)	86	74	62	72.09	83.78	82.23
Water	79	78	77	97.47	98.72	98.61
Totals	981	981	836			
Overall classification accuracy = 85.22%						
Overall k statistics = .8385						

ing materials (and is therefore spectrally similar). An additional level of complexity may also be present if both the residences and the commercial center use locally derived raw materials (river gravels for example) as landscaping cover. The latter example is illustrated by comparison of image reflectance spectra obtained from asphalt and river gravels located within the study area (Fig. 4). Road-grade asphalt usually contains approximately 95% aggregate comprised of sand- to gravel-sized minerals and rocks (Brown, McRae, & Crawley, 1989). This suggests that the two land covers would appear very similar spectrally to the TM sensor, and indeed, these two classes were highly confused using simple hard classifiers.

Some variability between intraclass training region reflectance signatures is evident from the standard deviations of the merged class means presented in Table 2. In such cases, it is preferable to use the individual intraclass training region signatures for classification rather than a merged signature. Application of the maximum likelihood decision rule to these intraclass training regions was precluded, however, as a Gaussian distribution of pixel values was not achieved (particularly for the disturbed classes). This is due to the small number of pixels available to define individual intraclass training regions for disturbed classes within the study area. Use of higher resolution, remotely sensed data could help to alleviate this difficulty by allowing the definition of "pure" training regions in urban areas with more robust statistics.

Inspection of the class training region means and standard deviations used in the initial maximum likelihood classification therefore reflect both subpixel mixing and merging of intraclass training regions (Table 2). Classes such as water and vegetation have well-defined band reflectance means that have relatively little overlap. However, this is not the case for the other classes that exhibit similar class mean reflectance values and standard deviations (disturbed xeric and mesic residential). This similarity of band reflectance values in the TM bandpasses indicates that considerable confusion between classes is inevitable using the spectral information alone. One approach to solving this problem was to employ a fuzzy classification algorithm. Fuzzy classifiers rank the probability of a given pixel's membership to defined classes (Foody, 2000). These rankings then can be used to generate a classification based on the most likely class a given pixel belongs to. Application of a fuzzy classifier to the study area improved accuracy somewhat using a four-class scheme, but did not significantly improve the overall accuracy of the eight-class scheme (Table 4). The degree of spectral overlap between classes evident in Table 2 indicates that similar distance rankings will be obtained for the majority of image pixels. Use of a fuzzy classification algorithm alone does not, therefore, provide a significant improvement in classification accuracy for the study area.

4.2. Incorporation of TM and ancillary data in the expert system model

The expert system was constructed to assign the greatest weight to the spectral information contained in the TM data (as represented by the initial classification results). This was done to maximize the temporal insensitivity of the model, as well as to minimize errors inherent in some of the ancillary data (such as the land use dataset). Additional information useful in class discrimination was provided by the replacement of the 120 m/pixel thermal infrared TM band with a vegetation index (Vogelmann et al., 1998). The spectral signature of vegetation in semiarid to arid environments tends to be dominated by soil reflectance, therefore the SAVI was chosen as being most appropriate for the conditions (Huete, 1988). Use of a band ratio such as SAVI also helped to alleviate shadow effects caused by topographic variations within the TM subscene.

Spatial texture derived from the TM subscene was included in the expert system as an additional postclassification variable. Regions with little to no texture (corresponding to alluvial fans, soil-mantled hill slopes, agricultural fields, and river channels) had pixel values less than 10 DN. Areas of intermediate to high texture (pixel values $\geq$ 10 DN) included natural (jointed outcrops, river channel banks, etc.) and man-made linear features (canals, roadways, etc.), as well as dense urban features such as residential, commercial, and industrial areas. These threshold DN values were determined by detailed inspection of texture image pixels corresponding to the land cover types of interest. These results are similar to those obtained by Gong and Howarth (1990) and Stuckens et al. (2000) for urban areas. The pixel resolution of the TM data precluded finer discrimination of the urban classes, therefore the texture information was used primarily to distinguish natural from urbanized regions during postclassification sorting. Incorporation of texture derived from higher resolution datasets (such as orthorectified digital aerial photographs) into the expert system might allow for greater discrimination of urban land covers.

The remaining ancillary datasets (land use, water rights, incorporated city and reservation boundaries) were all used in a postclassification sorting mode to reclassify the original maximum likelihood classification. The land use data were used primarily to correct misclassification errors between the undisturbed and urban classes caused by similar subpixel land cover components (vegetation and gravelly soils similar to desert landscaping). Land use data were also used to define the cultivated grass class as this vegetation type occurs mainly in golf courses and urban parks in the study region. The parameters used to generate the land use classification are in some cases not well constrained (J. Fry, personal communication), therefore no class assignments were made solely on the basis of the land use data. Incorporated city and Native American reservation boundary data were used primarily to distinguish urban from

nonurban classes. Areas of high vegetation density within reservation boundaries were observed to be in agricultural use throughout the study area. The water rights database does not extend to Native American reservations, so pixels with high SAVI values and low spatial texture values were reclassified as cultivated vegetation. Pixels within the reservation boundaries that were initially classified as compacted soil and had low spatial texture values were reclassified as compacted soil (prior agricultural use).

The water rights database includes information on areas that maintain active water use for agricultural purposes, as well as other water uses such as mining. This information, combined with vegetation density information (pixels classified as vegetation), allowed for reclassification of vegetated pixels as cultivated vegetation. An agricultural water right exists whether or not a particular field is active or fallow. Pixels originally classified as compacted soil were reclassified as compacted soil (prior agricultural use), if they were within an active agricultural water right area. The State of Arizona Groundwater Management Act of 1980 precludes the creation of any additional agricultural water rights from that time forward. Changes in water right status between 1980 and the present are therefore limited to conversion from agricultural to other nonagricultural uses. The times and nature of water right conversions are recorded at the ADWR, however, this historical information is not in a form useable by the expert system. The data available in GIS form from the ADWR reflect the current water rights status only. Use of the expert system model with earlier TM (or other sensor) data could potentially misclassify historically active and fallow agricultural regions as vegetation and compacted soil (respectively), if water right conversion took place after 1980. Strictly speaking, these classifications would still be correct, however, the interpreted land use would be incorrect.

4.3. Expert system results

Inspection of the accuracy assessment results presented in Table 5 indicates that all classes, with the exception of vegetation and disturbed (commercial/industrial), have user's accuracy and k values greater than 80%. These accuracy values are in good agreement with previous uses of expert class systems using TM data in urban regions (Greenberg & Bradley, 1997; Harris & Ventura, 1995; Stuckens et al., 2000; Vogelmann et al., 1998). The vegetation class has a user's accuracy of 72.62% ($k = 70.19\%$), and the disturbed (commercial/industrial) class has a user's accuracy of 49.30% ($k = 46.34\%$). The vegetation class is defined primarily by high SAVI values and high reflectance values in TM Band 4. The SAVI was designed specifically for use in arid regions to reduce the effect of soil reflectance on the vegetation signature (Huete, 1988). However, a high SAVI value may still be calculated in areas of sparse vegetation cover and high soil reflectance such as alluvial fans derived from silicic bedrock. This can lead to confusion with other classes having similar

properties (such as the undisturbed class). Addition of vegetation type and density information to the expert system would help to reduce this error.

The disturbed (commercial/industrial) class exhibits the worst performance of the classes used in the expert system. The subpixel land cover components comprising this class (Table 3) are also present in varying areal abundance within all of the other urban land cover classes. This similarity of subpixel land cover components leads to significant confusion with other classes. Comparison of misclassified pixels with the reference dataset and field data suggests that the error is primarily one of commission. As noted previously, the Phoenix metropolitan region is characterized by highly intermingled land cover types (both on the pixel and subpixel level) that are difficult to distinguish solely on the basis of reflectance spectra or spatial texture at TM resolutions. Incorporation of land use or zoning information into the expert system could improve the accuracy of the disturbed (commercial/industrial) class with the potential risk of introducing temporal and/or actual error (i.e. land zoned as residential that is undisturbed desert at the time of data acquisition).

5. Conclusions

The primary objective of the present work was to produce a useable classification of land cover types for the CAP LTER project and develop a methodology for similar studies at other urban centers around the world using ASTER. An expert system approach was used to meet this goal. Expert systems have been used to classify land cover in temperate urban centers, but this is perhaps the first such application of the method to a semiarid–arid urban center. Initial classification of the Phoenix, AZ metropolitan study area was performed using VSWIR band reflectance of 1998 Landsat TM data and SAVI values derived from the same dataset. Spatial texture was also calculated from the TM data and combined with ancillary datasets in the expert system to perform postclassification sorting of the initial land cover classification. Overall classification accuracy obtained using the expert system was 85%. Individual class user's accuracy ranged from 73–99%, with the exception of the disturbed (commercial/industrial) class (49%). The poor performance of this class is due to confusion with other classes stemming from the similarity of subpixel components at the scale of a TM pixel. The generally high user accuracies for the individual land cover classes validate the use of the expert system model approach for semiarid–arid urban centers.

A major strength of the expert system approach is in its flexibility with regard to data sources and potential for application to diverse research questions. The methodology described here will be used to monitor future land cover

changes in the CAP LTER study area using ETM+ and ASTER data. It will also be applied to ASTER data collected for over 100 global urban centers. The inherent flexibility of the expert system approach will allow both the increased spectral resolution available from ASTER and the varying amount of ancillary information available for each urban center to be used for land cover classification and monitoring.

Acknowledgments

References

ALRIS (1999). Arizona Land Resource Information System, Arizona State Land Department, Phoenix, Arizona.

Anderson, J. R., Hardy, E., Roach, J., & Witmer, R. (1976). A land use and land cover classification system for use with remote sensor data. U.S.G.S. Prof. Paper 964.

Bastin, L. (1997). Comparison of fuzzy c-means classification, linear mixture modeling and MLC probabilities as tools for unmixing coarse pixels. *International Journal of Remote Sensing*, 18, 3629–3648.

Berberoglu, S., Lloyd, C. D., Atkinson, P. M., & Curran, P. J. (2000). The integration of spectral and textural information using neural networks for land cover mapping in the Mediterranean. *Computers & Geosciences*, 26, 385–396.

Botkin, D. B., Estes, J. E., & MacDonald, R. B. (1984). Studying the earth's vegetation from space. *BioScience*, 34, 508–514.

Brown, E. R., McRae, J. L., & Crawley, A. B. (1989). Effect of aggregates on performance of bituminous concrete. In: H. G. Schreuders, & C. R. Marek (Eds.), *Implication of aggregates in the design, construction, and performance of flexible pavements* (pp. 34–62). Philadelphia, PA: American Society for Testing and Materials STP 1016.

Cibula, W. G., & Nyquist, M. O. (1987). Use of topographic and climatological models in a geographical data base to improve Landsat MSS classification for Olympic National Park. *Photogrammetric Engineering and Remote Sensing*, 53, 67–75.

Congalton, R. G., & Green, K. (1999). *Assessing the accuracy of remotely sensed data: principles and practices*. New York: Lewis Publishers.

ERDAS. (1999). *ERDAS field guide* (5th ed.). Atlanta, GA: ERDAS.

Fisher, P. F., & Pathirana, S. (1990). The evaluation of fuzzy membership of land cover classes in the suburban zone. *Remote Sensing of Environment*, 34, 121–132.

Foody, G. M. (2000). Estimation of sub-pixel land cover composition in the presence of untrained classes. *Computers & Geosciences*, 26, 469–478.

Franklin, S. E. (1994). Discrimination of subalpine forest species and canopy density using digital CASI, SPOT PLA and Landsat TM

data. *Photogrammetric Engineering and Remote Sensing*, 60, 1233–1241.

GEOSYSTEMS GmbH. (1997). *ATCOR2 for ERDAS Imagine user manual*. Germany: Germering.

Gong, P., & Howarth, P. J. (1990). The use of structural information for improving land-cover classification accuracies at the rural–urban fringe. *Photogrammetric Engineering and Remote Sensing*, 56 (1), 67–73.

Greenberg, J. D., & Bradley, G. A. (1997). Analyzing the urban–wildland interface with GIS. *Journal of Forestry*, 95, 18–22.

Haack, B. (1983). An analysis of Thematic Mapper Simulator data for urban environments. *Remote Sensing of Environment*, 13, 265–275.

Haack, B., Bryant, N., & Adams, S. (1987). An assessment of Landsat MSS and TM data for urban and near-urban land-cover digital classification. *Remote Sensing of Environment*, 21, 201–213.

Harris, P. M., & Ventura, S. J. (1995). The integration of geographic data with remotely sensed imagery to improve classification in an urban area. *Photogrammetric Engineering and Remote Sensing*, 61, 993–998.

Huete, A. R. (1988). A soil-adjusted vegetation index (SAVI). *Remote Sensing of Environment*, 25, 295–309.

Iron, J. R., & Petersen, G. W. (1981). Texture transforms of remote sensing data. *Remote Sensing of Environment*, 11, 359–370.

Jensen, J. R. (1996). *Introductory image processing: a remote sensing perspective* (2nd ed.). Upper Saddle River, NJ: Prentice-Hall.

Kumar, A. S., Basu, S. K., & Majumdar, K. L. (1997). Robust classification of multispectral data using multiple neural networks and fuzzy integral. *IEEE Transactions on Geoscience and Remote Sensing*, 35, 787–790.

Lindgren, D. T. (1985). *Land use planning and remote sensing*. Boston: Martinus Nijhhoff.

Lorenzo-Garcia, D. F., & Hoffer, R. M. (1993). Synergistic effects of combined Landsat-TM and SIR-B data for forest resources assessment. *International Journal of Remote Sensing*, 14 (14), 2677–2694.

Loveland, T. R., Merchant, J. W., Ohlen, D. O., & Brown, J. F. (1991). Development of a land-cover characteristics database for the conterminous U.S. *Photogrammetric Engineering and Remote Sensing*, 57, 1453–1463.

Lyon, J. G., Yuan, D., Lunetta, R. S., & Elvidge, C. D. (1998). A change detection experiment using vegetation indices. *Photogrammetric Engineering and Remote Sensing*, 64 (2), 143–150.

Maricopa Association of Governments. (1995). *MAG existing land use (1995) database*. Phoenix, AZ: Maricopa Association of Governments.

Martin, L. R. G., Howarth, P. J., & Holder, G. (1988). Multispectral classification of land use at the rural–urban fringe using SPOT data. *Canadian Journal of Remote Sensing*, 14 (2), 72–79.

Mattikalli, N. M. (1997). Soil color modeling for the visible and near-infrared bands of Landsat sensors using laboratory spectral measurements. *Remote Sensing of Environment*, 59, 14–28.

Paola, J. D., & Schowengerdt, R. A. (1995). A detailed comparison of back propagation neural networks and maximum likelihood classifiers for urban land use classification. *IEEE Transactions on Geoscience and Remote Sensing*, 33, 981–996.

Pax-Lenney, M., & Woodcock, C. E. (1997). The effect of spatial resolution on the ability to monitor the status of agricultural lands. *Remote Sensing of Environment*, 61, 210–220.

Quattrochi, D. A., & Ridd, M. K. (1998). Analysis of vegetation within a semi-arid urban environment using high spatial resolution airborne thermal infrared remote sensing data. *Atmospheric Environment*, 32 (1), 19–33.

Ramsey, M. S., Stefanov, W. L., & Christensen, P. R. (1999). Monitoring world-wide urban land cover changes using ASTER: preliminary results from the Phoenix, AZ LTER site. In: *Proceedings of the 13th International Conference, Applied Geological Remote Sensing*, vol. 2, (pp. 237–244). Ann Arbor, MI: ERIM International.

Ridd, M. K. (1995). Exploring a V-I-S (vegetation-impervious surface-soil) model for urban ecosystem analysis through remote sensing: comparative anatomy for cities. *International Journal of Remote Sensing*, 16, 2165–2185.

Ridd, M. K., & Liu, J. (1998). A comparison of four algorithms for change

detection in an urban environment. *Remote Sensing of Environment*, *63*, 95–100.

Stuckens, J., Coppin, P. R., & Bauer, M. E. (2000). Integrating contextual information with per-pixel classification for improved land cover classification. *Remote Sensing of Environment*, *71*, 282–296.

Sultan, M., Arvidson, R. E., Sturchio, N. C., & Guinness, E. A. (1987). Lithologic mapping in arid regions with Landsat Thematic Mapper data: Meatiq dome, *Geological Society of American Bulletin*, *99*, 748–762.

Treitz, P. M. (1992). Application of satellite and GIS technologies for land-

cover and land-use mapping at the rural–urban fringe: a case study. *Photogrammetric Engineering and Remote Sensing*, *58* (4), 439–448.

Vogelmann, J. E., Sohl, T., & Howard, S. M. (1998). Regional characterization of land cover using multiple sources of data. *Photogrammetric Engineering and Remote Sensing*, *64*, 45–57.

Wilkie, D. S., & Finn, J. T. (1996). *Remote sensing imagery for natural resources monitoring: a guide for first-time users*. New York: Columbia Univ. Press.